A Novel Harmonic Current Control Algorithm for Torque Ripple Reduction of Permanent Magnet Synchronous Motors for Traction Application

Amir Ebrahimi
Institute for Drive Systems and Power Electronics
Leibniz Universität Hannover
Hannover, Germany
ebrahimi@ial.uni-hannover.de

***Abstract*—This paper presents a novel control algorithm for high-torque low-speed permanent magnet synchronous motors for direct drive applications. A new induced voltage based formulation of the electromagnetic torque is developed and a novel current control algorithm is designed to reduce the torque ripples which are originated from the flux harmonics. A prototype motor with relatively high induced voltage harmonics is designed and constructed and the experiment results of the Harmonic control algorithm are compared to the results of a conventional Field Oriented Control.**

Keywords—control; torque ripple; traction; current harmonic; permanent magnet synhcronous motor

I. Introduction

With the growing of Electric Vehicle (EV) industry and direct drive applications the requirement of high performance, low torque ripple motors is growing rapidly. Permanent Magnet Synchronous Motor (PMSM) has been considered as a proper candidate for EV applications due to its compactness, high torque and dynamic, robustness and high efficiency. Considering the EV application not only a fast torque response is required but also a smooth performance with minimum torque ripple at low speed is essential. However, PMSMs usually show a considerable torque ripple if it is not compensated. Torque ripples due to the cogging torque, current torque, current measurement and flux harmonics restrict the application of the PMSMs [1], [2], [3], [4]. These torque ripples cause undesirable mechanical vibration at low speed [1]. This paper deals with the torque ripples which are originated from non-sinusoidal and asymmetrical back EMFs. The tolerances and limitations in design and manufacturing of an electrical motor lead to asymmetrical EMFs in three phases which can consequently lead to torque ripples [5]. Also the ferromagnetic components are typically driven near or above the saturation flux density at least at nominal load operation. This leads to non-sinusoidal linked fluxes in the stator coils and, hence, creates disruptive torque ripple during operation when the motor is fed with sinusoidal currents developed by Field Oriented Control (FOC) [6]. Several methods are proposed to deal with this pulsating torques. These methods can be categorized into two main groups. The first group includes methods which deal with the motor design aspects such as winding modification, skewing etc. However, the applicability of these techniques is limited to newly developed motors, and they can result in a further complicated realization and higher manufacturing cost [1]. The second type includes the optimization of control algorithm to deal with non-sinusoidal EMFs. Due to the non-sinusoidal linked fluxes and the therefrom caused non-constant torque during operation when using sinusoidal phase currents, the standard dq-transformation is not suitable for an accurate control. Some authors have used a modified dq-model in order to overcome this problem [6]. Another approach is developing a modified non-sinusoidal EMF model of PMSM using dependent voltage and current sources [7]. Another similar approach is developing a back-stepping model of the motor [8]. It is also possible to calculate the actual non-sinusoidal air gap flux density distribution using extended Kalman filter [9]. Furthermore, the phase asymmetries are considered using recursive least square method [5]. There are also different efforts to reduce the torque pulsation by modification the control algorithm. An iterative learning control algorithm for torque ripple reduction caused by stator saturation is proposed in [6] and [1]. Predicative control for torque ripple reduction using the derivative of the currents is discussed in [10]. In [11] a closed-loop control strategy is developed to suppress the circulation of zero sequence currents and amplitude of the dominant current harmonics caused by the non-sinusoidal EMFs. The zero sequence component is considered as one additional degree of freedom that has to be managed. A method based on the third harmonic current to improve the torque performance of a five phase PMSM is discussed in [12]. Reference [13] uses the speed harmonic by a proper injection of current harmonics into the motor for the direct calculation of maximum torque per ampere angle. Variable frequency methods are also addressed in some works [14]. The advantages of using instantaneous voltage control technique for torque ripple reduction in PMSM are discussed in [15]. Time error signals are generated directly from the different phase voltages. In [16] the abilities of pseudo derivative feedback controller to improve the performance of PMSMs at standstill and low speed regions are discussed. A predictive current control for torque ripple reduction of a PMSM with variable switching frequency is addressed in [17]. The proposed control scheme is based on a FOC and optimizes the switching frequency on each sample. However, many authors suggest the modification of Direct Torque Control to reduce the torque ripple [18], [19]. Reference [20] considers the asymmetry of a six phase motor and design a modified DTC to deal with that. Another possibility to receive a low torque ripple is to make use of higher harmonics in the stator phase currents [6].

This paper presents a control algorithm which energizes the motor with three phase non-sinusoidal currents to compensate the non-sinusoidal EMFs. The motor torque formulation is derived using output active power principal and the current controller is designed to generate a very smooth torque at low speed. A motor prototype with a non-sinusoidal EMF is constructed and the control algorithm is validated using an electromechanical test bench.

II. ELECTROMAGNETIC TORQUE FORMULATION

The conventional FOC is based on the assumption of a sinusoidal phase flux linkage and currents. Benefiting from sinusoidal electrical properties, the park transformation can be used and the FOC can be applied. However, this is not always the case. The harmonics of the induced voltage cause the torque pulsation. The electromagnetic torque of a PMSM can be calculated using induced voltage.

$$P = T\omega = E_a I_a + E_b I_b + E_c I_c \tag{1}$$

P, *T* and *ω* are the output power, torque and rotational speed of the motor and E_i and I_i are the three phase EMFs and currents. Considering the total harmonics of currents and the derivation of fluxes and describing them using the Fourier series, we can achieve a more general form of the torque. It is supposed that the normalized induced voltages and the current are odd and symmetric as it is always the case in PMSM. Thus the general equation of the motor active power can be formulated as the multiplication of phase currents and induced voltages. This is given by:

$$\begin{aligned} T\omega = &\left[\sum_{m=1}^{\infty} B_m \sin(m\theta)\right]\left[\sum_{n=1}^{\infty} A_n \sin(n\theta)\right] \\ &+\left[\sum_{m=1}^{\infty} B_m \sin(m\theta - m\frac{2\pi}{3})\right]\left[\sum_{n=1}^{\infty} A_n \sin(n\theta - n\frac{2\pi}{3})\right] \\ &+\left[\sum_{m=1}^{\infty} B_m \sin(m\theta + m\frac{2\pi}{3})\right]\left[\sum_{n=1}^{\infty} A_n \sin(n\theta + n\frac{2\pi}{3})\right] \end{aligned} \tag{2}$$

A_n and B_m are the harmonic amplitudes of currents and induced voltages. In the case of $n=m$ the first part of the power equation is given by:

$$\begin{aligned} T\omega = &\sum_{n=1}^{\infty} A_n B_n \sin^2(n\theta) + \sum_{n=1}^{\infty} A_n B_n \sin^2\left(n\theta - n\frac{2\pi}{3}\right) \\ &+ \sum_{n=1}^{\infty} A_n B_n \sin^2\left(n\theta + n\frac{2\pi}{3}\right) = \sum_{n=1}^{\infty} \frac{A_n B_n}{2}\left[3 - \cos(2n\theta)\right. \\ &\left. - \cos\left(2n\theta - \frac{4n\pi}{3}\right) - \cos\left(2n\theta + \frac{4n\pi}{3}\right)\right] \end{aligned} \tag{3}$$

In the case of $n \neq m$ the other term of the power is given by:

$$\begin{aligned} T\omega = &\sum_{m=1}^{\infty}\sum_{n=1}^{\infty} A_n B_m \sin(n\theta)\sin(m\theta) + \\ &\sum_{m=1}^{\infty}\sum_{n=1}^{\infty} A_n B_m \sin\left(n\theta - \frac{2n\pi}{3}\right)\sin\left(m\theta - \frac{2m\pi}{3}\right) + \\ &\sum_{m=1}^{\infty}\sum_{n=1}^{\infty} A_n B_m \sin\left(n\theta + \frac{2n\pi}{3}\right)\sin\left(m\theta + \frac{2m\pi}{3}\right) \end{aligned} \tag{4}$$

Both terms of power which are indicated in the equation (3) and (4) include zero terms which can be eliminated and the power can be given by:

$$\begin{aligned} T\omega = &\sum_{\substack{n=1 \\ \{n\neq 3k \\ n=m}}^{\infty} \frac{3A_n B_n}{2} - \sum_{\substack{n=1 \\ \{n=3k \\ n=m}}^{\infty} \frac{3A_n B_n}{2}\cos(2n\theta) \\ &+ \sum_{\substack{m=1 \\ n\neq m}}^{\infty}\sum_{n=1}^{\infty} \frac{A_n B_m}{2}\left\{\cos(m-n)\theta + \cos\left[(m-n)\theta + (n-m)\frac{2\pi}{3}\right]\right. \\ &\left. + \cos\left[(m-n)\theta + (m-n)\frac{2\pi}{3}\right]\right\} \\ &- \sum_{\substack{m=1 \\ n\neq m}}^{\infty}\sum_{n=1}^{\infty} \frac{A_n B_m}{2}\left\{\cos(m+n)\theta + \cos\left[(m+n)\theta - (n+m)\frac{2\pi}{3}\right]\right. \\ &\left. + \cos\left[(m+n)\theta + (m+n)\frac{2\pi}{3}\right]\right\} \end{aligned} \tag{5}$$

It can be simply shown that in the case of sinusoidal currents and EMFs the famous torque formulation of PMSM can be achieved from equation (5) [21]. Once the order and the amplitude of harmonics of induced voltage are determined, the order and amplitude of current are computed in order to result in a constant torque. The general block diagram of the control algorithm is indicated in Fig. 1.

III. HARMONIC CURRENT CONTROLLER

The reference values of the three phase currents are calculated by the current estimator unit shown in Fig. 1. The current estimator unit receives the harmonics of the three phase induced voltages as well as cogging torque as inputs. These values are functions of motor position and speed. The reference value of the torque is computed by the speed control loop which can also be arbitrarily realized. The main part of the proposed control algorithm is the current estimator unit. It predicts the three reference currents of the three phases. The current calculation depends on the order and amplitude of the harmonics of the induced voltage. It is clear that the higher order harmonic terms require a very fast response of the current controller which due to the limited current and voltage capability of the power electronic device and predefined values of the motor inductances is not always realizable. The EMF harmonic spectrum of the prototype motor is indicated in Fig. 2 [22]. The functionality of the current estimator is described by assuming the 1th and 11th harmonics of the induced voltage. Now taking a look at the equation (5) it is possible to select the order of the current harmonics. It can easily be deduced with a good compromise between complexity and realizeability that the current should include the 1st and 11th harmonics. Now these known B_1 and B_{11} and unknown A_1 and A_{11} are put into the equation (5) and the rest of coefficients are set to zero.

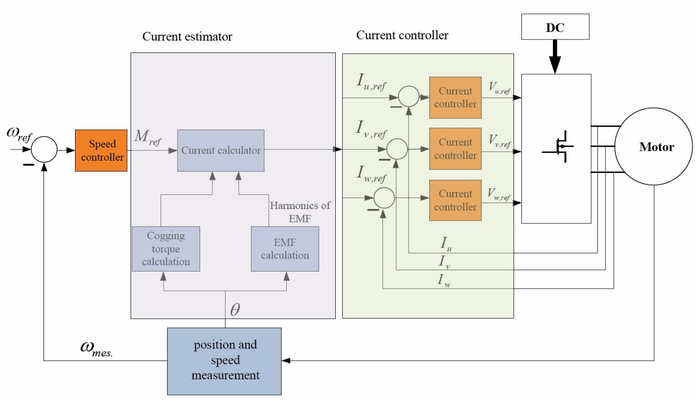

Fig. 1. Block Diagram of the control algorithm

Hence, according to the equation (5) the power is given by:

$$T\omega = \frac{3}{2}[(A_1B_1 + A_{11}B_{11}) - (A_{11}B_1 + A_1B_{11})cos12\theta] \quad (5)$$

The torque consists of a constant and a position dependent term including the 12th harmonic. The term corresponding to the 10th harmonic is eliminated automatically. Therefore, the amplitude and order of the current harmonics term can be determined to eliminate the position dependent term. This leads to a system of equations given by:

$$\begin{cases} A_1B_1 + A_{11}B_{11} = \frac{2}{3}T\omega \\ A_{11}B_1 + A_1B_{11} = 0 \end{cases} \quad (6)$$

A_1 and A_{11} are calculated in each step and sent as the reference value of current to the current controller. Supposing a pure open loop torque controller, the reference value of torque is sent to the current estimator in case of the proposed controller. The optimized current references are calculated based on equation (6). However, in the case of FOC, the reference value of i_q is estimated based on the park transformation and the current is sent to the corresponding current controller [23].

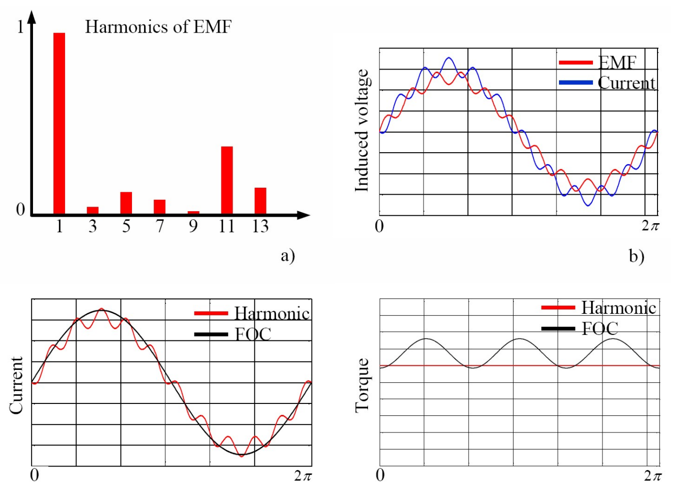

Fig. 2. Simulation results of proposed control algorithm, a) harmonics of EMF, b) EMF and currents of one phase of the motor, c) comparison between the current waveform of FOC and Harmonic controller, d) comparison between the torque waveform of FOC and Harmonic controller

The simulation results are indicated in Fig. 2. The novel algorithm method explained in section II is indicated as Harmonic in Fig. 2. For the simplicity of the calculation, it is assumed that the EMF includes only the 1st and the 11th harmonics. An exaggerated 11th harmonic of the induced voltage is deliberately assumed in order to emphasize the effectiveness of the proposed control algorithm. As it can be observed, the current form is determined exactly complementary to the non-smoothness of the induced voltage. This consequently results into a smooth torque as it is indicated in Fig. 2. The FOC on the other side develops a pure sinusoidal current which results into ripples in the torque behavior across the rotor angle. Using this method, it is theoretically possible to eliminate all harmonics of the torque. However, the time constant of the current, the reaction time of the current controller and the switching time of the power electronic device are not ideally zero. Therefore, it is practically impossible to eliminate the higher ripples of the torque. Thus, this method is particularly suitable for low speed motors.

IV. PROTOTYPE AND EXPERIMENTAL TEST BENCH

To verify the proposed control algorithm a two kilowatt PMSM was designed and constructed which is indicated in Fig. 3. The prototype is designed with high measurable harmonics in induced voltage. The stator consists of 168 laminated silicium iron sheet with thickness of 0.5 millimeter and 24 slots which are holding the 3 phase windings. There are 2 windings per pole per phase [24]. Therefore, each phase consists of 4 coils which are switched in series and each of them includes 6 teeth. The magnets are NdFeB type N35 with maximum working temperature of 80 Celsius. There are four poles at rotor with 60 degree pole pitch. Each pole realized using 9 pieces of cubic magnets with parallel magnetization which are indicated in Fig. 4. Considering the prototype construction of Fig. 3, it is clear that the flux density in the air gap is not pure sinusoidal. The magnets are stuck to the rotor using two components metal glue. The green cables at rotor and stator are the thermal elements for temperature monitoring. Since the maximum speed of the motor is below 3000 round per minute, it is not necessary to use extra bandage to protect the magnets. To compare the calculated and the measured values of flux density in the air gap, there are overall six thin hall sensors which are mounted on teeth and slots which can be seen in Fig. 3. Their circuits are printed on an ultra-thin flexible PCB with thickness of 0.05 millimeter. So it is possible to install the hall sensors in the 1mm air gap. There are 3 magnets in axial directions for each phase and to monitor all of 36 magnets of rotor, 3 hall sensors are mounted axially in the air gap on teeth and 3 of them are mounted in the slots. This configuration facilitates the measuring of the asymmetry and inequality of magnets.

The prototype is mounted on an experimental test with 3-phase power electronics, dSPACE control system, torque gauge and a braking machine. The three phase power electronic realized using power Mosfets with independent gate control [25], [26]. The FOC and harmonic control are realized using dSPACE control unit.

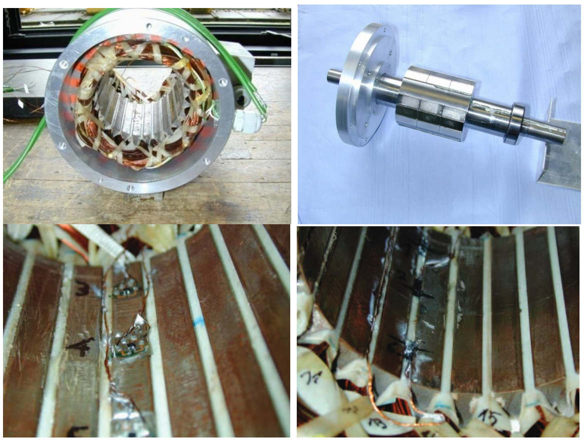

Fig. 3. The PMSM prototype with hall sensors mounted in the air gap

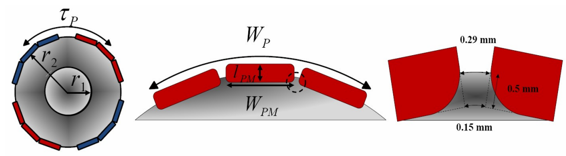

Fig. 4. Rotor structure of the prototyped motor with permanent magnets

V. Experimental Results

Both the FOC and the Harmonic controller of section III are realized using the experimental test bench. An exact model of the motor is simulated using MATLAB/Simulink. The simulated model includes different look-up tables for an exact modeling of the motor behaviors. The look-up tables simulate the position and current dependent inductances, the induced voltages and cogging torque based on the measurements. Both the FOC and the Harmonic controller are modelled in dSPACE and the simulated and experimental results are compared to each other for each controller. The three phase currents of the simulated motor and the experimental results of the prototype are indicated in Fig. 5. Since there are several mechanical terms such as frictions, coupling, and mechanical resonance of the experimental test bench, there is a small deviation between the emulator and experimental results of speed.

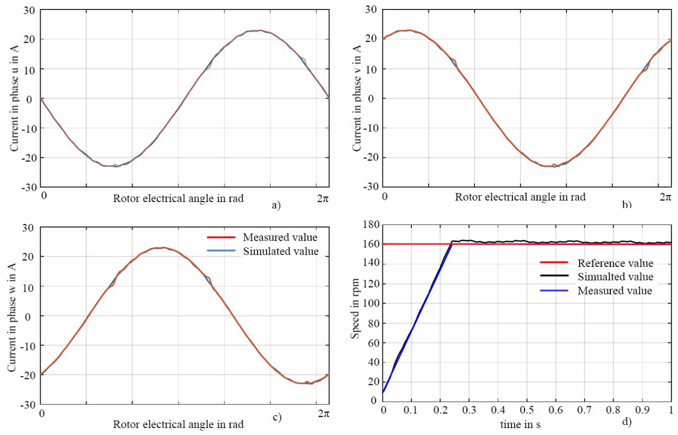

Fig. 5. Comparison of FOC results; simulated motor vs. experimental results a) current in phase u, b) current in phase v, c) current in phase w, d) speed

The experimental results of the novel control algorithm of section III are indicated in Fig. 6. The current controller successfully follows the reference values sent from the current estimator. Determination of the parameters of the speed loop is based on the rotation equation consisting of speed, torque and moment of inertia. The moment of inertia can be determined by a set of measurements. Thanks to the proposed control algorithm the electromagnetic torque is predicted almost exactly but the non-electromagnetic torques, such as friction and wind loss or cogging torque are indeterminate parameters within speed control loop. These values can be switched off manually or with the help of an observer. The current control loop depends only on the electrical components of each phase such as self and mutual inductivities, resistance and induced voltage.

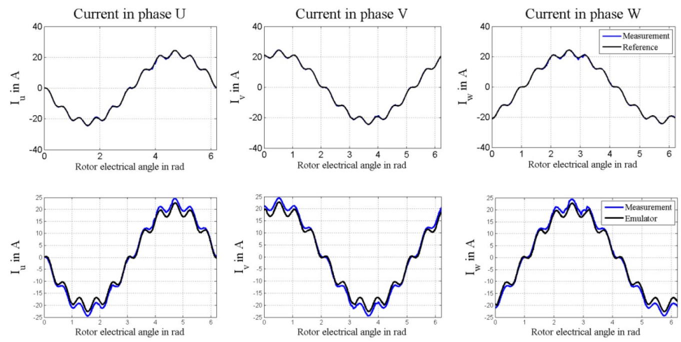

Fig. 6. Current control loop; top: The measured current and its reference value in all three phases, bottom: Comparison between measured value and simulation

The controller assumes a constant inductance for each phase and neglects their current and position dependencies. These non-zero components of the electrical loop can also be considered for the determination of control parameters and switched off using a variety of different methods. However, the induced voltage of each phase is switched off manually using a preset look-up table. Since the control algorithm has to deal with non-sinusoidal motor properties, the induced voltage should either be switched off manually as it is done here or rather it can be modeled mathematically and considered by the design of controller. Through the implementation of a current loop controller with a simple hysteresis controller, facing these problems is automatically avoided. However, current ripples demand a very high sampling frequency and a variable switching frequency which is a disadvantage of this method. From the experimental results one can see that the FOC is a little faster than the harmonic controller. The reason is the higher energy of current wave form of FOC than that of the Harmonic controller. However, the difference is negligibly small.

VI. Conclusion

A novel motor control approach is introduced in this paper to reduce the EMF-harmonic based torque ripple of PMSMs. The control algorithm actively calculates the amplitude of current harmonics to generate a constant torque. The proposed control algorithm is best proper for in-wheel traction motors with non-ideal flux linkages and EMFs. Compared to a conventional FOC, the proposed algorithm generates a constant torque despite of the motor non-sinusoidal EMF. This motor control approach based on the real torque behavior leads to new ideas in the design of PMSMs. There are varieties of applications which need a periodic torque-speed characteristic. This is usually realized by applying a conventional motor and an enhanced control algorithm which can follow a specific torque-speed curve. Beyond this solution, it is also possible to design a motor which naturally performs a desired torque behavior over different rotor positions. Torque is already demonstrated as a function of induced voltage and current. Theoretically any desired torque characteristic can be realized by a smart selection of the appropriate form of induced voltage and current. It is also possible to design motors with non-trivial yet controllable torque characteristics.

REFERENCES

[1] J. Liu, H. Li, Y. Deng, "Torque Ripple Minimization of PMSM on Robust ILC Via Adaptive Sliding Mode Control," *IEEE Trans. Power Electronics*, vol. 33, no. 4, pp. 3655-3671, Apr. 2018.

[2] W. Qian, S. K. Panda, and J.-X. Xu, "Torque ripple minimization in PM synchronous motors using iterative learning control," *IEEE Trans. Power Electronic*, vol. 19, no. 2, pp. 272–279, Mar. 2004.

[3] J. A. Guemes, A. A. Iraolagoitia, J. J. DelHoyo, P. Fernandez, "Torque analysis in permanent-magnet synchronous motors: A comparative study," *IEEE Trans. Energy Convers.*, vol. 26, no. 1, pp. 55–63, Feb. 2011.

[4] A. Gebregergis, M. Chowdhury, M. Islam, T. Sebastian, "Modeling of permanent magnet synchronous machine including torque ripple effects," *IEEE Trans. Ind. Appl.*, vol. 51, no. 1, pp. 232–239, Jan. 2015.

[5] Y. Xu, N. Parspour, U. Vollmer, "Torque Ripple Minimization for PMSM using Online Estimation of the Stator Resistances," *XXth International Conference on Electrical Machines*, pp. 1107-1113, Sep. 2012, Marseille, France.

[6] G. Bramerdorfer, W. Amrhein, S. Lanser, "PMSM for high demands on low torque ripple using optimized stator phase currents controlled by an iterative learning control algorithm," *39th Annual Conference of the IEEE Electronics Society*, pp. 8488-8493, Nov. 2013, Vienna, Austria.

[7] M. Pronin, O. Shonin, A. Vorontsov, G. Gogolev, "A Control System-based Reduction of Electromagnetic Torque Ripples in a VSI-Fed Poly-Phase PMSM with Non-Sinusoidal Back-EMF," *IEEE EUROCON*, pp. 990-995, May 2009, St.-Petersburg, Russia.

[8] J. Xu, J. Zhao, W. Gu, Y. Wang, "An Optimal Direct Torque Control System Based on Backstepping Model,“ *29th Chinese Control and Decision Conference*, pp. 5046-5051, May 2017, Chongqing, China.

[9] X. Xiao, C. Chen, "Reduction of Torque Ripple Due to Demagnetization in PMSM Using Current Compensation," *IEEE Trans. Applied Superconductivity*, vol. 20, no. 3, pp. 1068-1071, Jun. 2010.

[10] X. Xiao, C. Chen, "Reduction of Torque Ripple Due to Demagnetization in PMSM Using Current Compensation," *IEEE Trans. Applied Superconductivity*, vol. 20, no. 3, pp. 1068-1071, Jun. 2010.

[11] N. Said, M. Priestly, R. Dutta, J. Fletcher, "Torque ripple minimization in dual inverter open-end winding PMSM drives with non-sinusoidal back-EMFs by harmonic current suppression," *42nd Annual Conference of the IEEE Industrial Electronics Society*, pp. 2975-2980, Oct. 2016, Florence, Italy.

[12] Z. L. Zong, K. Wang, J. Y. Zhang, "Control Strategy of Five-Phase PMSM Utilizing Third Harmonic Current to Improve Output Torque,“ *Chinese Automation Congress*, pp. 612-6117, Oct. 2017, Jinan, China.

[13] C. Lai, G. Feng, , J. Tjong, N. C. Ka, "Direct Calculation of Maximum-Torque-per-Ampere Angle for Interior PMSM Control Using Measured Speed Harmonic," *IEEE Trans. Power Electronics*, in press.

[14] F. Ramirez, M. Pacas, "Enhanced Control of the Torque Ripple in a PMSM Drive with Variable Switching Frequency," *19th European Conference o Power Electronics and Applications*, PP. 1-10, Sep. 2017, Warsaw, Poland.

[15] K. Raj Kumar, K. Nithin, T. Vinay Kumar, "Torque Ripple Reduction in PMSM Drive based on Instantaneous voltage Control Technique," *7th Power India International Conference*, pp. 1-6, Nov. 2016, Bikaner, India.

[16] A. Karthikeyan, K. K. Prabhakaran, B. Venkatesa Perumal, Nagamani, „Pseudo Derivative Feedback current controlled sensorless PMSM drive with Flux-Torque based MRAS estimator for low speed operation," *IEEE International Symposium on Sensoreless Control for Electrical Drives*, pp. 115-120, Sep. 2017, Catania, Italy.

[17] F. Ramirez-Figueroa, M. Pacas, "Model Based Control of a PMSM with Variable Switching Frequency and Torque Ripple Control," *41st Annual Conference of the IEEE Industrial Society*, pp. 1418-1423, Nov. 2015.

[18] M. H. Vafaie, B. M. Dehkordi, P. Moallem, and A. Kiyoumarsi, "Minimizing Torque and Flux Ripples and Improving Dynamic Response of PMSM Using a Voltage Vector With Optimal Parameters," *IEEE Trans. Ind. Electronics*, vol. 63, no. 6, Jun. 2016.

[19] S. Yavuz, A. Echle, N. Parspour, „Control Strategy for a Direct Torque Control of a Switched reluctance Motor," XXII International Conference on Electrical Machines (ICEM), pp. 1008-1014, Sep. 2016.

[20] X. Wang, Z. Wang, P. Liu, M. Cheng, "A Hybrid Direct Torque Control Scheme for Asymmetric Six-Phase PMSM Drives," *43rd Annual Conference of the IEEE Industrial Electronics Society*, pp. 1686 – 1691, Oct. 2017, Beijing, China.

[21] A. Ebrahimi, Hybrid Analytical Modeling and Optimization of Surface Mounted Permanent Magnetic Synchronous Motors Considering Spatial Harmonics, Aachen: Shaker. Berichte aus dem Institut für Elektrische Energiewandlung 6, ISBN 978-3-8440-5026-4, 2016.

[22] A. Ebrahimi, "Analytical Modeling of Permanent Magnetic Synchronous Motors Considering Spatial Harmonics," *Brazilian Power Electronic Conference, COBEP 2017*, pp. 1-6, Nov. 2017, Juiz de Fora, Brazil.

[23] A. Ebrahimi, M. Maier, N. Parspour, „Analysis of Torque Behavior of Permanent Magnet Synchronous Motor in Field-Weakening Operation,“ *Power and Energy Conference at Illinois (PECI), IEEE Conference Publications*, pp. 120-124, Feb. 2013, Illinois USA.

[24] A. Ebrahimi, N. Parspour, "Modified analytical modeling of surface mounted permanent magnet synchronous motor- design and prototype tests," *4th International Conference on Power Engineering, Energy and Electrical Drives* , pp. 12-18, May 2013, Istanbul Turkey.

[25] A. Ebrahimi, N. Parspour, M. Fabian, "Design and qualitative thermographic comparison of different power inverter packaging," *4th International Conference on Power Engineering, Energy and Electrical Drives*, pp. 401-404, May 2013, Istanbul Turkey.

[26] A. Ebrahimi, F. Dreher, N. Parspour, „Sensorless direct torque control of transverse flux machines with hybrid flux conduction,“ *International Conference on power conversion und intelligent motion, PCIM*, 2013, Nuremberg, Germany.